CHEMIJA. 2013. Vol. 24. No. 4. P. 279–287

Preparation of hydrophilic TiO_2 films by chemical solution deposition

Edita Garškaitė*

Department of Inorganic Chemistry,
Faculty of Chemistry,
Vilnius University,
Naugarduko St. 24,
LT-03225 Vilnius,
Lithuania

In this work homogeneous and crack-free titanium dioxide (TiO_2) films were grown by chemical solution deposition on fluorine doped tin oxide (FTO) glass substrates. The influence of solution composition and deposition time on films morphology was investigated. Morphological features of deposited TiO_2 films were characterized by scanning electron microscopy. Raman spectroscopy studies and peak deconvolution analysis showed that annealed at 500 °C TiO_2 films possess an anatase crystal structure. Measurements of a contact angle of water revealed that the surface of the FTO glass after the deposition of TiO_2 films became more hydrophilic (contact angle decreased by 45° ± 5). Furthermore, after the irradiation with UV light the contact angle was further reduced from 26 to 7° and from 34 to 13° for films deposited in 2 and 4 h, respectively.

Key words: titanium dioxide (TiO_2), chemical solution deposition, scanning electron microscopy, Raman spectroscopy, hydrophilicity

INTRODUCTION

Titanium dioxide (TiO_2) is a wide bandgap (E_g = 3.0–3.2 eV) ultraviolet (UV) sensitive, but chemically stable semiconductor. It also possesses a high refractive index and an excellent optical transmittance. Owing to these properties TiO_2 is used for various applications including paints, sunscreens, solar cells, water and air purification, and self cleaning coatings [1–4]. In general, self cleaning coatings depending on their contact angle can be divided into two broad categories: hydrophobic – with surfaces having a contact angle higher than 90°, and hydrophilic – with a contact angle of less than 90°. On hydrophobic surfaces the drop of water rolls out of the surface and so removes the dirt with it, while on hydrophilic surfaces water spreads over it becoming a layer which carries away the dirt. A self-cleaning feature of TiO_2 coatings is their combination of hydrophilicity and photocatalitic activity. Upon the UV light irradiation on the surface of TiO_2 free electron-hole pairs are generated which further contribute to the adsorption of reactant species and various redox reactions on the gas-solid and liquid-solid interfaces. When hydrophilicity process dominates over photocatalysis, the reduction of Ti^{4+} to Ti^{3+} cations takes place and photogenerated holes oxidize the O_2^- anions. Further, –OH groups having a very high affinity towards water are formed so that H_2O molecules occupy a thin layer of space, and a hydrophobic surface is turned into a hydrophilic one. Combination of these processes allows for the environmental contaminants to be removed easily from the TiO_2 surface and subsequently extends the durability of the material [4–6].

To deposit TiO_2 films a variety of physical and chemical deposition methods were used. Techniques such as atomic layer deposition (ALD) [7, 8], sputtering [9, 10], pulsed laser deposition (PLD) [11], liquid flame spray (LFS) [12, 13] and metalo-organic chemical vapor deposition (MOCVD) [14] require costly setup. Also, when high vacuum system or high temperatures are used during the deposition process, a control of stoichiometry, morphology, particle size and uniformity of films might be more difficult to achieve.

* Corresponding author. E-mail: edita.garskaite@gmail.com

As alternatives, some solution based techniques like sol-gel [15–17], adsorptive self assembly [18] or chemical bath deposition (CBD) [19] provide several advantages such as being less costly and allowing a good control over these parameters at relevantly low synthesis temperatures. Moreover, these processing conditions affect the porosity and crystal phase structure of the material and these subsequently strongly influence the hydrophilicity of the coating. Table 1 gives a brief summary on the various processing methods used to deposit TiO_2 films, annealing temperature, obtained crystal phase and values of contact angles of water measured from these films. On can tell that optimization of parameters to produce uniform nanocrystalline films with well defined hydrophilic properties remains still an issue to be improved.

The objective of this work was to prepare TiO_2 films by chemical solution deposition and investigate their hydrophilic properties. The effect of solution composition and deposition time on the morphology of TiO_2 films was studied. The hydrophilic behaviour of deposited films before and after UV irradiation was obtained and is discussed herein.

EXPERIMENTAL

Synthesis of the colloidal solution

Titanium (IV) oxysulfate ($TiOSO_4 \cdot nH_2O$, 29% TiO_2, Sigma-Aldrich), acetic acid (CH_3COOH, 99.8%, Acros Organics), sulphuric acid (H_2SO_4, 95–98%, Sigma-Aldrich) and ammonium acetate (CH_3COONH_4, Riedel-de-Haën) were used to prepare TiO_2 containing colloidal solution. Firstly, 0.7996 g (0.005 mol) of $TiOSO_4 \cdot nH_2O$ was dispersed in a solution containing 40 mL of distilled water and 1 mL of CH_3COOH by vigorously stirring at 60 °C for 15 min in a beaker covered with a watch glass. Then, 2 mL of H_2SO_4 were supplied to the solution to adjust pH and control hydrolysis and condensation reactions. The prepared mixture was further stirred for 20 min until a clear and transparent solution was obtained. In the following step, 0.154 g (0.002 mol) of CH_3COONH_4 was added to associate sulphate ions in the prepared solution, and the obtained mixture was further stirred at 60–65 °C for 30 min. A necessary amount of distilled water was then supplied so that the total volume of the solution was 50 mL. The pH of the prepared solution was adjusted to 0.5 by adding H_2SO_4. The finally obtained colloidal solution was stirred at 65 °C for 30 min.

Deposition of films

The fluorine doped tin oxide (SnO_2 : F, FTO) glass plates (Pilkington, USA) were used as substrates. Before the deposition the substrates were cleaned in acetone, deionised water and 96% ethanol under sonication for 30 min in each solvent.

To produce TiO_2 films the FTO glass substrates (size of 1×3 cm^2) were immersed into the beaker with the prepared colloidal solution and kept covered with a watch glass. During deposition the solution was continuously stirred with a magnetic stirrer. A deposition time of 2, 4 and 8 h was used. Afterwards, the grown films were dried at room temperature for 24 h and then heat treated in a single continuous run at 110 °C (for 10 min), 125 °C (15 min), 325 °C (5 min), 375 °C (5 min), 450 °C (5 min) and 500 °C (15 min) with a heating rate 5 °C/min.

Characterisation

UV-Vis absorbance spectrum of the colloidal solution was recorded using an Ultrospec 2100pro UV/Visible Spectrometer (GE Healthcare, Ltd.). The spectra of prepared solutions were measured 4 h after their preparation. The particle size of the prepared solutions was measured with a Zetasizer Nano ZS90 (Malvern Instruments Ltd.) using dynamic light scattering (DLS). The surface morphology and elemental composition of the deposited films were investigated with a JSAM-6500F (JOEL, Ltd.) field emission scanning electron microscope (FE-SEM) equipped with an energy dispersive X-ray spectrometer (EDX). The electron beam accelerating voltage was 15 kV for SEM and EDX analysis. Raman spectra were recorded using a Micro Raman MonaRa 500i Spectrophotometer (Omicron laser controlled software 532 nm laser, Gratings 1200) (DongWoo Optron Co., Ltd.) in 90° scattering configuration. Raman peak fitting and deconvolution was carried out by the OriginPro 8 software (OriginLab Coorporation). Hydrophilicity was evaluated by water contact angle measurements using a FTA 1000 B Surface Analyser (First Ten Angstroms Inc.). Contact angle measurements were conducted on three points for each sample. A hand help Hg UV light lamp (maximum intensity at 254 nm) was used as an illumination source.

RESULTS AND DISCUSSION

Evaluation of the colloidal solution

The UV-Vis absorption spectrum of the TiO_2 solution was recorded 2 h after its preparation. In Fig. 1 the presented spectrum shows that the TiO_2 solution had no absorbance in the visible range (400–600 nm) and that the absorption band edge was at around 360–370 nm. Similar results of the absorption band edge were obtained by Kolar et al. when formed surface complexes of TiO_2 and 2-coumarin acid were investigated [27].

It can be mentioned that a series of experiments was performed when solutions with a higher concentration of CH_3COONH_4 were prepared. However, an increased amount of CH_3COONH_4 led to a formation of precipitate in a relatively short time. Reduced stability of the colloidal solution could be explained by the change in pH value. This induces higher nucleation rates of primary particles which further aggregate to form a larger particle. Conversely, when a solution was prepared without CH_3COONH_4, no growth of films was obtained under the same experimental conditions.

A particle size of the colloidal solution measured before films deposition was estimated to be ~820 nm.

Table 1. **Summary of measured contact angles of water on TiO_2 films produced by various methods**

Deposition method	Crystal structure of TiO_2	Calcination temperature of TiO_2 films	Particle size / analysis method	Illumination time	Contact angle before UV illumination (°)	Contact angle after UV illumination (°)	Reference
Adsorptive self-assembly	anatase	400 °C	5–9 nm/TEM	–	60–70 (prior heat-treatment)	<5	[18]
Anodizing (AZ), thermal oxidation (TO), anodizing-thermal oxidation (ATO)	anatase (AZ and ATO), rutile (TO)	298 K (AZ), 673 K (TO and ATO)	n. r.	n. r.	n. r.	28–66	[20]
ALD	anatase and rutile	250, 350 °C	n. r.	15 and 30 min	~30–75	~2–75 (depend on thickness, annealing temp. and illumination time)	[7]
Combination of cold plasma treatment (CPT) and sol-gel dip-coating	anatase	393 K	n. r.	15 min	75 (with CPT) and 69 (without CPT)	5 (with CPT) and 30 (without CPT)	[21]
Dip-coating (from suspension)	anatase	no annealing	pillars with an average diameter of 179 nm/SEM	90 min	130	<5	[22]
Electrospinning	anatase	500 °C	rice grain-like structures (150 to 300 nm length and 100 to 200 nm diameter) consisting of spherical particles (15–20 nm)/SEM and TEM	n. r.	43	2 ± 1–17.5 ± 2	[23]
Liquid flame spray (LFS)	anatase	150 °C	40–80 nm/SEM and AFM	10–30 min	161	20 (after 10 min), 6 (after 30 min)	[12]
LFS	n. r.	450 °C	n. r.	186 h	45	<1 (after 8 h)	[13]
Liquid phase deposition (LPD)	amorphous	no annealing	0.5–1 μm/AFM	5 min	66	<1	[24]
MOCVD	anatase	400, 500 °C	n. r.	Coating 1, 2 and 3 : 10, 50 and 100 min, respectively	Coating 1, 2 and 3 : 15, 40 and 75, respectively	0	[14]
Plasma-enhanced ALD	anatase	250, 300 °C	n. r.	0–40 min	35	5 (after 20 min)	[8]
Pulsed dc reactive magnetron sputtering	anatase	400 °C	n. r.	5–60 min	~73 ~65	~10 (after 5 min) ~7 (after 60 min)	[10]
Radio frequency magnetron sputtering	amorphous	n. r.	n. r.	up to 80 min	~64	~4	[9]
Sol-gel dip-coating	anatase	500 °C	n. r.	up to 148 h	55	11 (after 2 h) and 0 (after 24 h)	[15]
Sol-gel dip-coating	anatase	450 °C	5–10 nm/XRD	24 h	48	≤5 (after few hours)	[17]
Sol-gel – evaporation-induced self-assembly (EISA)	anatase (mesoporous)	350–700 °C	7.6–12.7 nm/XRD	5 min	22 (600 °C)	~18 (600 °C)	[25]
Sparking	anatase / rutile	250, 500 and 700 °C	26–36 nm/SEM	n. r.	10.4	5.2 (250 °C), 2.5 (500 °C) and 7.8 (700 °C)	[26]

n. r. – not reported.

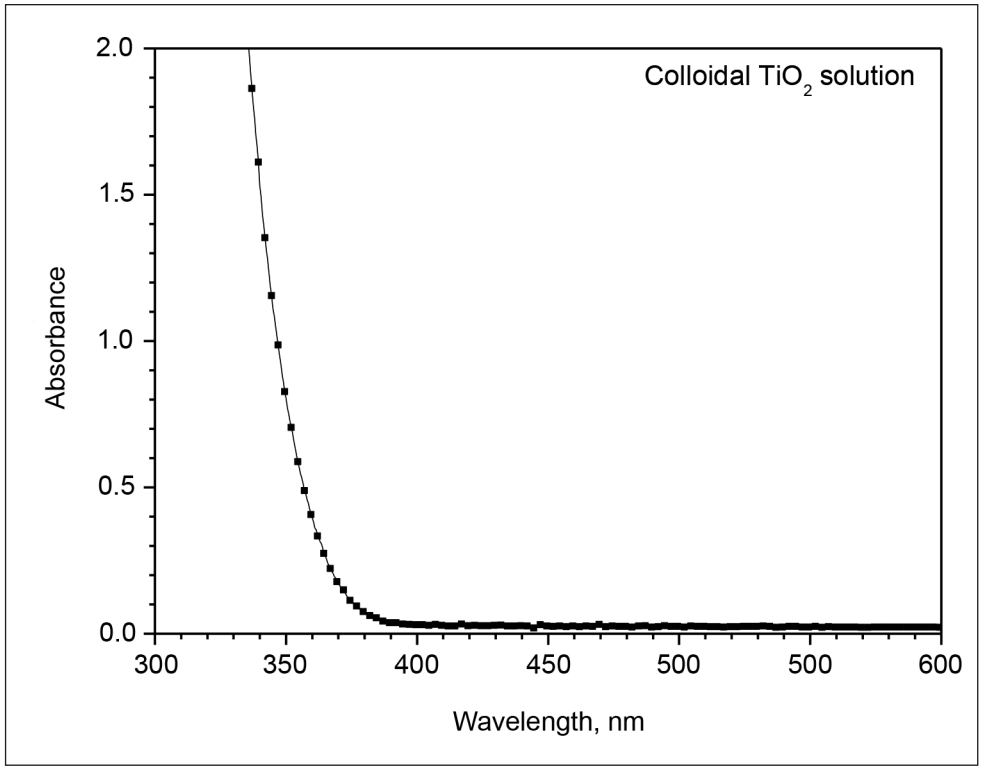

Fig. 1. UV-Vis absorbance spectrum of the colloidal TiO_2 solution

Morphology and elemental composition of films

Figure 2 shows FE-SEM micrographs of the calcined TiO_2 films deposited in 2 and 4 h. It can be seen that films annealed at 500 °C are crack-free and homogeneous with particles having a spherical shape. Furthermore, deposited films did not peal off from the substrate. This indicates good adhesion strength between the substrate and deposited film. Micrographs also show that surface texturing is more pronounced in the films deposited in 4 h (Fig. 2b). Such texturing might be influenced by several factors such as temperature of the solution, changes in the pH, deposition time and stirring rate. Also, the actual morphology of the FTO substrate might impact on the topography of the film. Such surface influenced patterning was demonstrated by Masuda and Kato where TiO_2 films were deposited by the liquid phase deposition method [28].

The average particle size of annealed films was estimated to be 15 ± 2 nm (FE-SEM micrographs).

The FE-SEM image and EDX spectrum of the TiO_2 film deposited in 4 h and annealed at 500 °C is presented in Fig. 3. In the EDX spectrum the elements of Ti, O, C, Sn and F were obtained. Sn and F elements were attributed to the substrate used, while C was attributed to the environmental impurities. Attention was also paid to other elemental impurities. No trace of S element was obtained which shows successful hydrolysis and condensation reactions in the solution preparation and film deposition processes.

Crystalline composition of films

The crystalline composition of deposited films was evaluated using Raman spectroscopy. The Raman spectrum of the TiO_2 film deposited in 4 h and sintered at 500 °C is presented in Fig. 4.

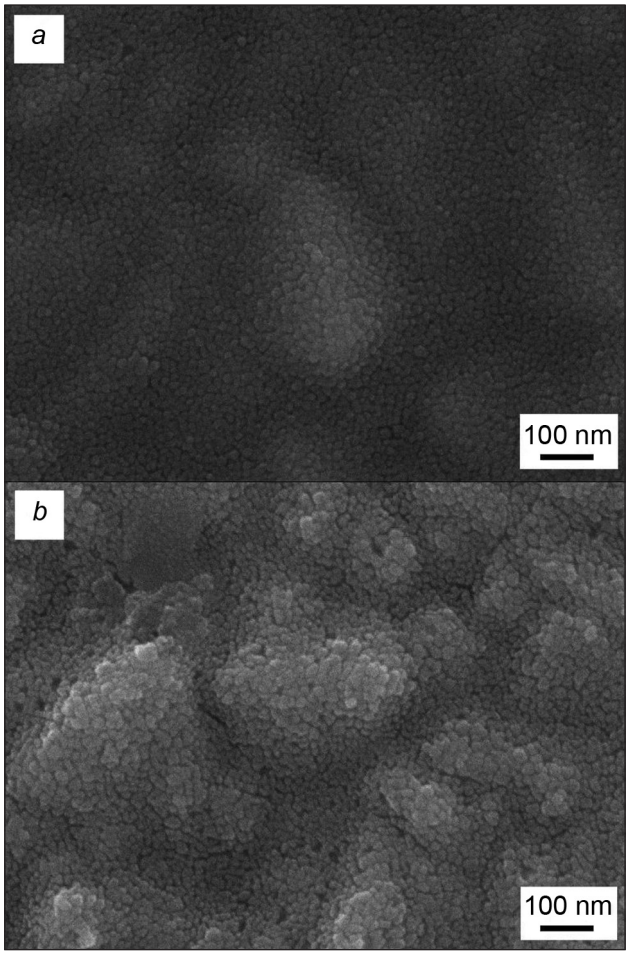

Fig. 2. FE-SEM micrographs of TiO_2 films deposited in 2 h (*a*) and 4 h (*b*) (annealed at 500 °C)

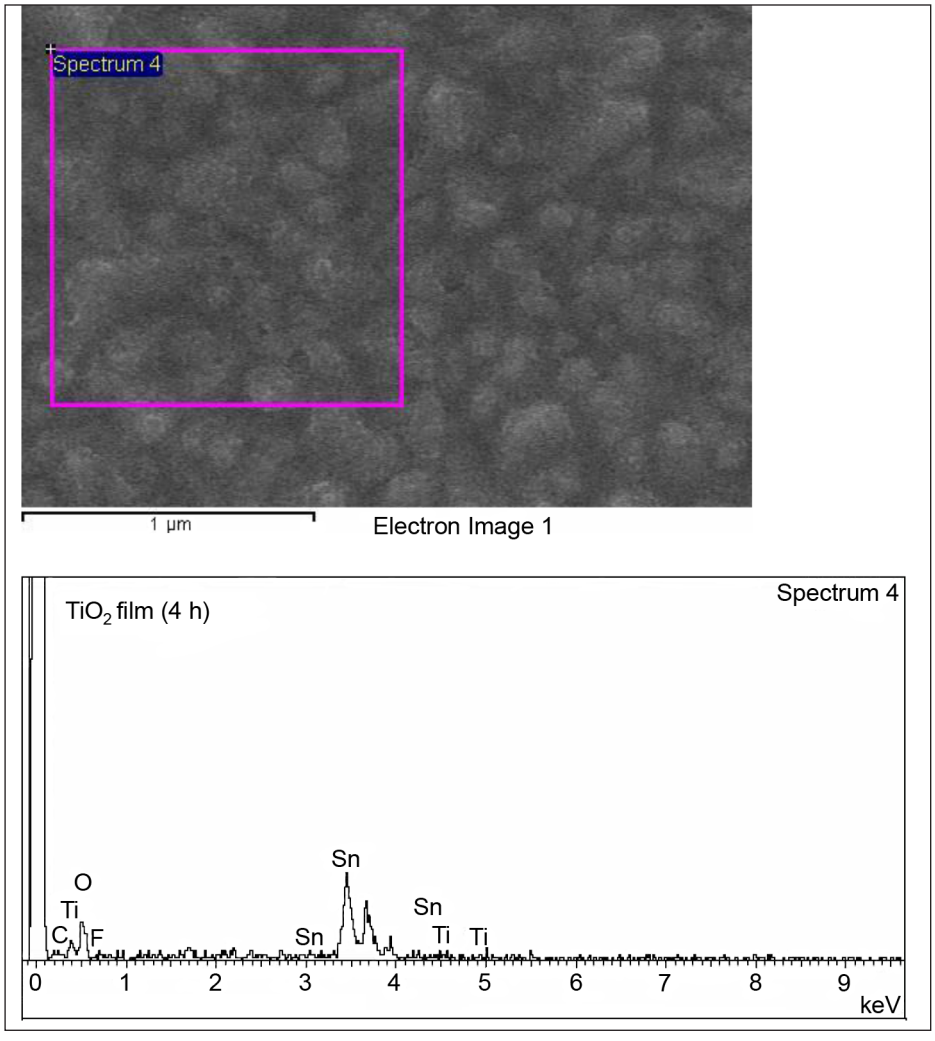

Fig. 3. FE-SEM micrograph and EDX spectrum of the TiO_2 film deposited in 4 h (annealed at 500 °C)

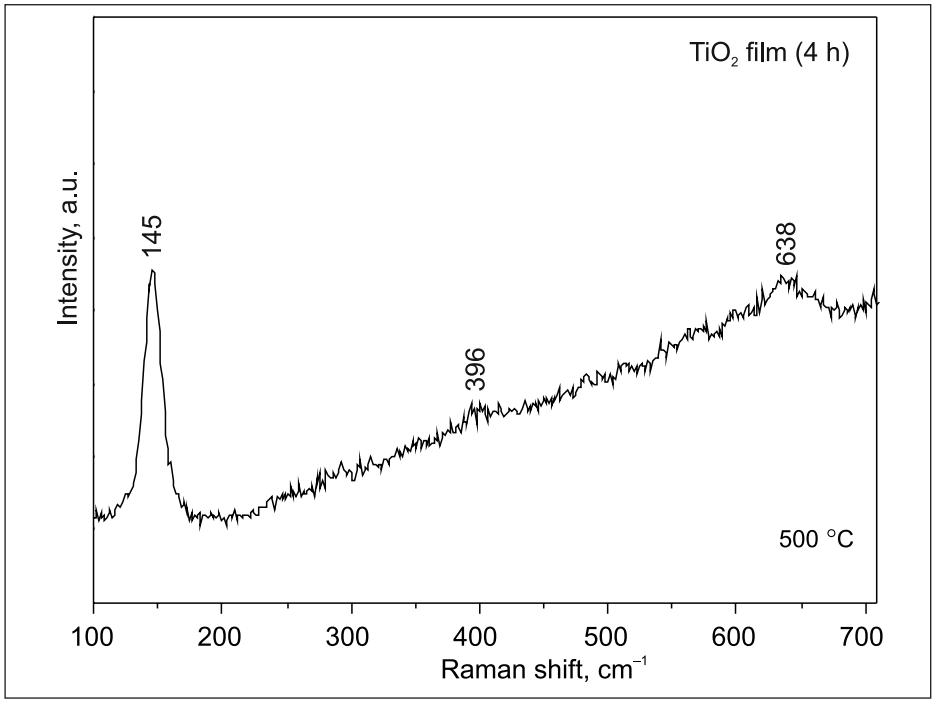

Fig. 4. Raman spectrum of the TiO_2 film deposited in 4 h (annealed at 500 °C)

The most prominent peak was observed at 145 cm^{-1} and assigned to the E_g mode coming from Raman active Ti-O lattice vibrations of the anatase TiO_2 [11, 29, 30]. Also, two weak peaks were obtained at 396 and 638 cm^{-1} and assigned to the B_{1g} and E_g modes coming from the anatase TiO_2 lattice vibrations [29]. A spectrum of the film deposited in 2 h was not recorded due to the film transparency and ultra-thin structure.

For comparison, the Raman spectrum from an opaque TiO_2 reference film deposited in 8 h (Fig. 5) was recorded. The significant vibrational modes characteristic to the anatase TiO_2 located at 145 cm^{-1} (E_g), 195 cm^{-1} (weak) (E_g), 396 cm^{-1} (B_{1g}), 517 cm^{-1} (A_{1g} and B_{1g}), and 638 cm^{-1} (E_g) were obtained in the spectrum. There were no additional peaks present in the spectrum corresponding to the rutile phase of TiO_2 that has Raman active modes at 144 cm^{-1} (B_{1g}), 446 cm^{-1} (E_g), 610 cm^{-1} (A_{1g}) and 827 cm^{-1} (B_{2g}) [29].

Additionally, a peak-fitting and deconvolution analysis of the Raman spectrum of the TiO_2 film deposited in 8 h was performed. It was reported that the ratio of the integrated Raman peak intensity of rutile at 446 cm^{-1} to that of anatase at 396 cm^{-1} may be used as a semi-quantitative measure of the weight ratio of rutile to anatase [29]. Thus, the peak located at 396 cm^{-1} was examined. Obtained results showed (Fig. 6a) that this peak consisted of one Lorentzian component centered at 396 cm^{-1}. Furthermore, the peak located at 638 cm^{-1} was examined confirming that there is no overlap with the 610 cm^{-1} band coming from the rutile TiO_2 (Fig. 6b). One can also find that no peaks located at ~440, 580 and 680 cm^{-1} were obtained where characteristic vibrations from amorphous TiO_2 normally appear [29]. Raman data and curve fitting analysis showed that TiO_2 films sintered at 500 °C possess an anatase crystal structure.

Hydrophilic properties of films

The surface wettability was investigated by measuring the contact angle θ of water. Images of the contact angles of the water drop deposited directly on the uncoated FTO glass and on the TiO_2 films after 5 min UV illumination are shown in Fig. 7,

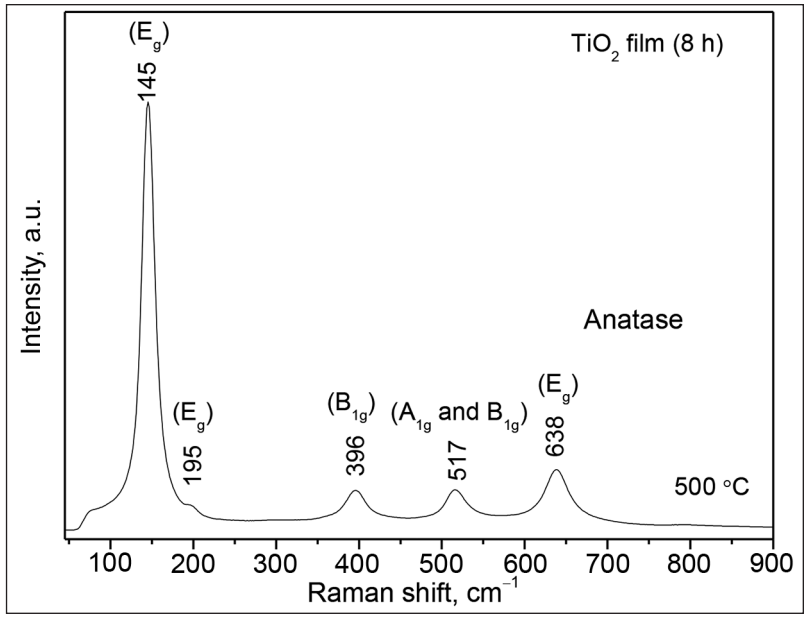

Fig. 5. Raman spectrum of the TiO_2 reference film deposited in 8 h (annealed at 500 °C)

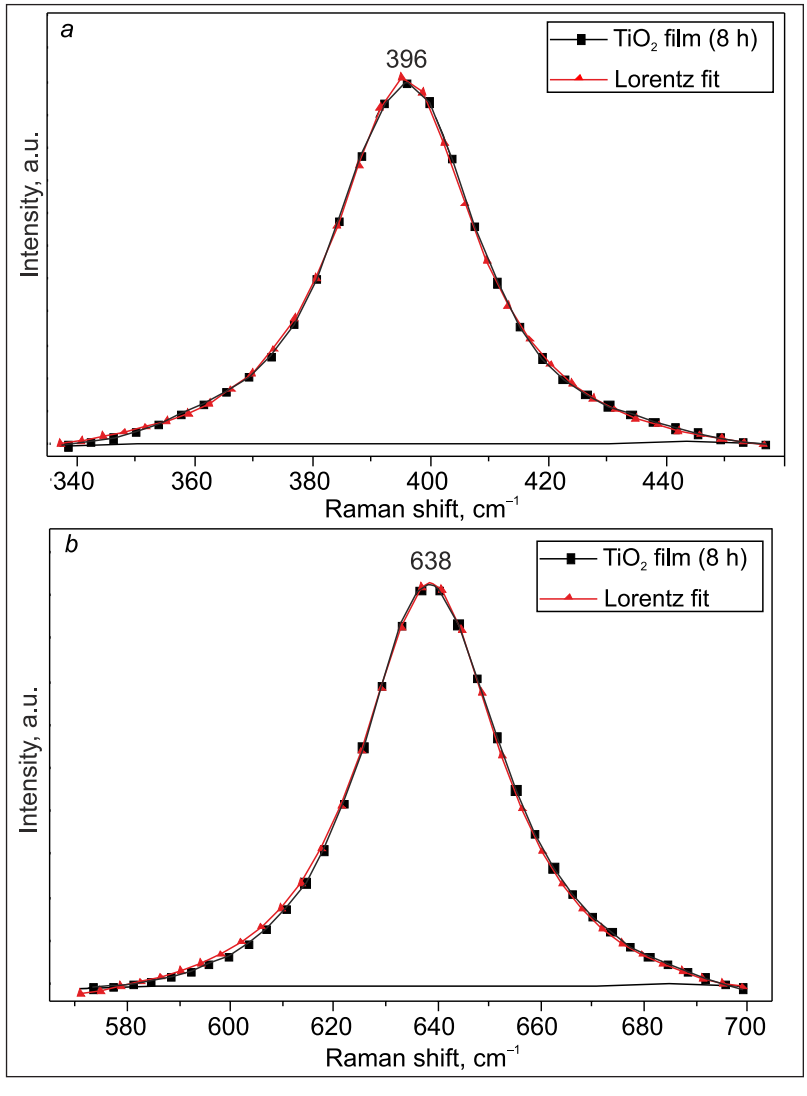

Fig. 6. Deconvolution of the two Raman peaks at 396 cm^{-1} (*a*) and 638 cm^{-1} (*b*) of the TiO_2 film deposited in 8 h. The peak deconvolution was performed using the Lorentz function

Table 2. **Values of the contact angle of water measured on the deposited TiO_2 films**

Deposition time	Contact angle (°)			
	Averaged before UV irradiation	5 min after UV illumination	5 min after removing UV illumination	15 min after removing UV illumination
2 h	26 ± 3	7.5	15.44	26.20
4 h	31 ± 3	13.39	21.79	34.38

while values of contact angles measured before and after the UV illumination are listed in Table 2. The average value of the contact angle measured on FTO glass was 75 ± 10°. Results showed that after the deposition the contact angle decreased from 75° to 26° for TiO_2 films grown in 2 h, whereas films grown in 4 h induce reduction of the contact angle to 34°. Such difference in contact angle values might be due to the roughness of the grown film which appears when deposition time is prolonged. Furthermore, after illumination for 5 min with UV light the contact angles were further decreased to 7° and 13° for films grown in 2 and 4 h, respectively. The standard deviation for contact angle measurements was from 0.5 to 2.9° (for obtained contact angles in receding order). After 30 min that the UV irradiation has been removed, the films almost regain their initial properties. The fast regeneration of the contact angle to its initial value might be induced by a short UV illumination time. Also, the factors such as surface morphology, surrounding temperature and the adsorption of air contaminants might influence its faster return to the initial state.

Further, the solid surface tension from the measured contact angle of water was calculated. In general, the solid surface tension can be calculated using the Young equation:

$$\gamma_{lv} \cdot \cos\theta = \gamma_{sv} - \gamma_{sl}, \tag{1}$$

where γ_{lv}, γ_{sv} and γ_{sl} are the interfacial tensions of the liquid-vapor, solid-vapor and solid-liquid interfaces, respectively. The only measurable quantities in the Young equation are γ_{lv} and θ. To obtain γ_{sv} and γ_{sl} additional relation is required. Therefore, in this work solid surface tension was calculated using Antonow's and Berthelot's rules combined with the Young equation [31]. Thus, combining the former rule with Young's equation yields

$$\cos\theta = -1 + 2\frac{\gamma_{sv}}{\gamma_{lv}}, \tag{2}$$

and a combination of Berthelot's rule with Young's equation and free energy of adhesion of a solid-liquid system gives

$$\cos\theta = -1 + 2\sqrt{\frac{\gamma_{sv}}{\gamma_{lv}}}. \tag{3}$$

A detailed description on the determination of the solid surface tension from contact angles using Antonow's and Bertholet's rules can be found elsewhere [31–33].

Calculated γ_{sv} values of the FTO glass and deposited TiO_2 film surfaces before and after the illumination with UV light

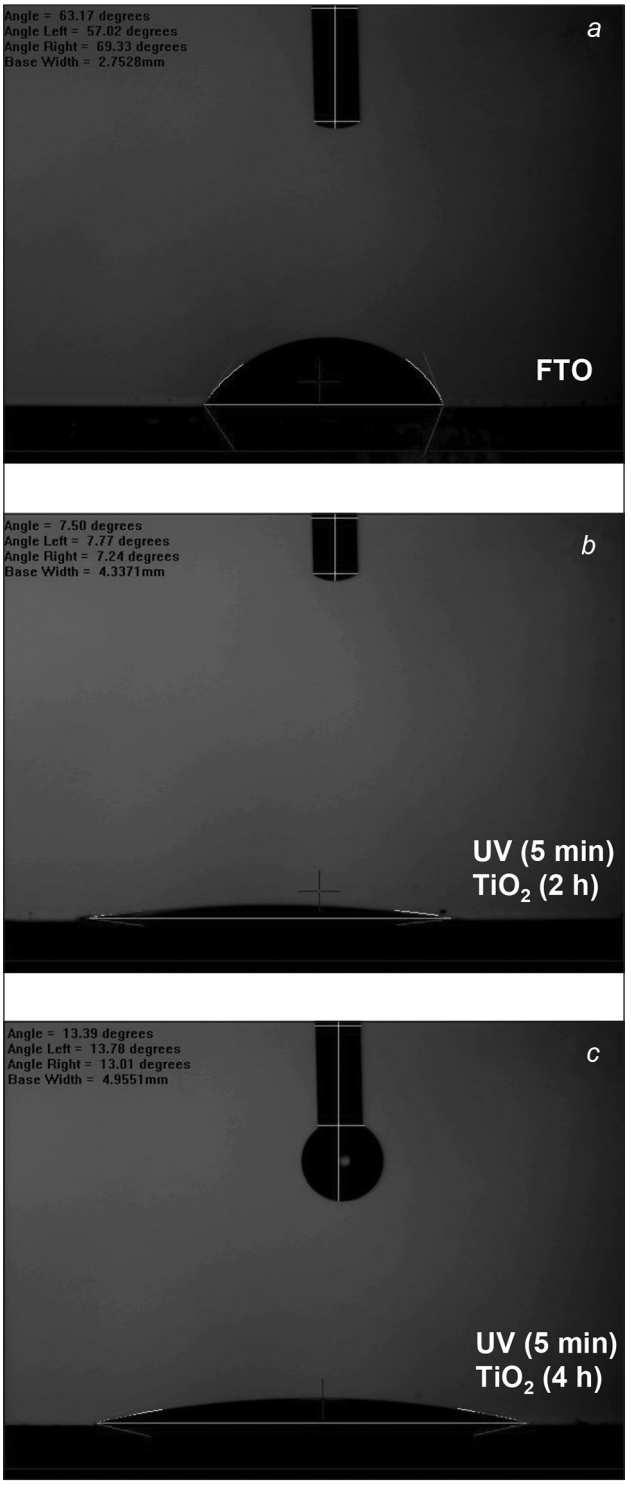

Fig. 7. Water contact angles measured on FTO glass (*a*) and annealed TiO_2 films after 5 min UV irradiation (deposited in 2 (*b*) and 4 h (*c*))

Table 3. **Calculated solid surface tension γ_{sv} values of the FTO glass and deposited TiO_2 film surfaces before and after the illumination with UV light from Antonow's and Berthelot's rules**

Material	Contact angle (°)	Solid surface tension (mN/m) Antonow's rule, Eq. (2)	Solid surface tension (mN/m) Berthelot's rule, Eq. (3)
FTO glass	63	52.92	38.42
TiO_2 film (2 h)	26	68.99	65.46
TiO_2 film (4 h)	31	67.50	62.67
TiO_2 film (2 h) (5 min after UV illumination)	7	72.40	72.11
TiO_2 film (4 h) (5 min after UV illumination)	13	71.75	70.81

are presented in Table 3. Obtained values show that γ_{sv} is higher when θ is smaller. Further, comparing the values calculated from Equations (2) and (3) one can see that differences among the solid surface tensions of TiO_2 films become more significant when the contact angle increases. Obviously, this is due to the way of handling the components of the equation to determine the solid surface tension. Furthermore, when conditions of $\gamma_{lv} \approx \gamma_{sv}$ or $\gamma_{lv} < \gamma_{sv}$ are fulfilled, complete wetting occurs. Obtained results from contact angle measurements agree with the conditions provided above.

The γ_{lv} of water of 72.7 mN/m was used to calculate γ_{sv} [34].

In this work it was shown that by carefully controlling the solution composition and deposition parameters it is possible to produce hydrophilic nanocrystalline TiO_2 films without the presence of other phases, by employing this simple chemical solution deposition route.

CONCLUSIONS

Homogeneous and crack-free TiO_2 films were grown by chemical solution deposition on the FTO glass substrates using $TiOSO_4 \cdot nH_2O$ as the starting material. The scanning microscopy analysis revealed that the surface texturing was more pronounced when the deposition time was prolonged. The Raman spectroscopy studies and peak deconvolution analysis showed that films sintered at 500 °C possessed an anatase crystal structure. Contact angle measurements showed that after the deposition of TiO_2 films the surface of the FTO glass became more hydrophilic. Furthermore, after the irradiation with UV light for 5 min the contact angle of water was further reduced from 26 to 7° and from 34 to 13° for films deposited in 2 and 4 h, respectively.

ACKNOWLEDGEMENTS

The study was funded from the European Community's Social Foundation under Grant Agreement No. VP1-3.1-SMM-08-K-01-004/KS-120000-1756. The National Taipei University of Technology is greatly acknowledged for providing an access to the instruments used to characterize prepared samples.

Received 13 June 2013
Accepted 31 July 2013

References

1. M. Hadnadjev, J. Ranogajec, S. Petrovic, S. Markov, V. Ducman, R. Marinkovic-Neducin, *Philos. Mag.*, **90**, 2989 (2010).
2. V. Shapovalov, *Glass Phys. Chem.*, **36**, 121 (2010).
3. B. O'Regan, M. Gratzel, *Nature*, **353**, 737 (1991).
4. K. Nakata, A. Fujishima, *J. Photochem. Photobiol. C*, **13**, 169 (2012).
5. A. Vincento, L. Vittorio, P. Mario, P. Giovanni, P. Leonardo, *Clean by Light Irradiation. Practical Applications of Supported TiO_2*, The Royal Society of Chemistry, Cambridge, UK (2010).
6. A. Fujishima, T. N. Rao, D. A. Tryk, *J. Photochem. Photobiol. C*, **1**, 1 (2000).
7. M. L. Kääriäinen, D. C. Cameron, *Surf. Sci.*, **606**, L22 (2012).
8. C.-S. Lee, J. Kim, G. H. Gu, et al., *Thin Solid Films*, **518**, 4757 (2010).
9. L. Sirghi, Y. Hatanaka, *Surf. Sci.*, **530**, L323 (2003).
10. M. Horprathum, P. Eiamchai, P. Limnonthakul, et al., *J. Alloy. Compd.*, **509**, 4520 (2011).
11. M. M. Shirolkar, D. Phase, V. Sathe, J. Rodriguez-Carvajal, R. J. Choudhary, S. K. Kulkarni, *J. Appl. Phys.*, **109**, 123512 (2011).
12. M. Stepien, J. J. Saarinen, H. Teisala, et al., *Surf. Coat. Tech.*, **208**, 73 (2012).
13. J. A. Pimenoff, A. K. Hovinen, M. J. Rajala, *Thin Solid Films*, **517**, 3057 (2009).
14. H. Y. Lee, Y. H. Park, K. H. Ko, *Langmuir*, **16**, 7289 (2000).
15. M. Piispanen, L. Hupa, *Appl. Surf. Sci.*, **258**, 1126 (2011).
16. H. Choi, A. C. Sofranko, D. D. Dionysiou, *Adv. Funct. Mater.*, **16**, 1067 (2006).
17. R. Fateh, A. A. Ismail, R. Dillert, D. W. Bahnemann, *J. Phys. Chem. C*, **115**, 10405 (2011).
18. B. Xi, L. K. Verma, J. Li, et al., *ACS Appl. Mater. Interf.*, **4**, 1093 (2012).
19. U. M. Patil, S. B. Kulkarni, P. R. Deshmukh, R. R. Salunkhe, C. D. Lokhande, *J. Alloy. Compd.*, **509**, 6196 (2011).
20. D. Yamamoto, I. Kawai, K. Kuroda, R. Ichino, M. Okido, A. Seki, *Bioinorg. Chem. Appl.*, **2012**, 7 (2012).
21. J. Zhuang, S. Weng, W. Dai, P. Liu, Q. Liu, *J. Phys. Chem. C*, **116**, 25354 (2012).
22. K. Nakata, M. Sakai, T. Ochiai, T. Murakami, K. Takagi, A. Fujishima, *Langmuir*, **27**, 3275 (2011).
23. V. A. Ganesh, A. S. Nair, H. K. Raut, T. M. Walsh, S. Ramakrishna, *RSC Adv.*, **2**, 2067 (2012).

24. Y. Gao, Y. Masuda, K. Koumoto, *Langmuir*, **20**, 3188 (2004).
25. J. Wang, H. Li, H. Li, C. Zuo, H. Wang, *J. Phys. Chem. C*, **116**, 9517 (2012).
26. W. Thongsuwan, T. Kumpika, P. Singjai, *Curr. Appl. Phys.*, **11**, 1237 (2011).
27. M. Kolář, H. Měšťánková, J. Jirkovský, M. Heyrovský, J. Šubrt, *Langmuir*, **22**, 598 (2005).
28. Y. Masuda, K. Kato, *Thin Solid Films*, **516**, 2547 (2008).
29. F. D. Hardcastle, *J. Ark. Acad. Sci.*, **65**, 43 (2011).
30. T. Ohsaka, F. Izumi, Y. Fujiki, *J. Raman Spectrosc.*, **7**, 321 (1978).
31. H. Tavana, A. W. Neumann, *Adv. Colloid Sci.*, **132**, 1 (2007).
32. D. Y. Kwok, A. W. Neumann, *Coll. Surf. A*, **161**, 31 (2000).
33. D. Cwikel, Q. Zhao, C. Liu, X. Su, A. Marmur, *Langmuir*, **26**, 15289 (2010).
34. N. B. Vargaftik, B. N. Volkov, L. D. Voljak, *J. Phys. Chem. Ref. Data*, **12**, 817 (1983).

Edita Garškaitė

HIDROFILINIŲ TITANO DIOKSIDO DANGŲ SINTEZĖ CHEMINIO NUSODINIMO METODU

S a n t r a u k a

Homogeniškos TiO_2 dangos buvo gautos cheminio nusodinimo būdu ant F:SnO_2 dengtų stiklo padėklų iš tirpalų, kurių ruošimui pradinė medžiaga – $TiOSO_4 \cdot nH_2O$. Tirpalo sudėtis ir padengimo laikas buvo keičiami norint nustatyti šių parametrų įtaką dangų morfologijai. Dangų morfologiniai ypatumai ir dalelių dydis tirti skenuojančia elektronine mikroskopija. Ramano spektroskopijos analizė ir gautų spektrų smailių intererogramos parodė, kad iškaitintoms 500 °C temperatūroje TiO_2 dangoms būdinga anatazo kristalinė struktūra. Atlikus vandens kontaktinio kampo matavimus nustatyta, kad padengus TiO_2 dangas labiau išryškėjo naudotų padėklų hidrofilinės savybės (kontaktinis kampas sumažėjo 45° ± 5). Taip pat nustatyta, kad TiO_2 dangas, paveikus 5 min. UV spinduliuotės šaltiniu, vandens kontaktinis kampas sumažėjo nuo 26 iki 7°, kai dangų padengimo laikas truko 2 val., ir nuo 34 iki 13°, kai dangų padengimo laikas – 4 val.